In vitro selection of RNA-based irreversible inhibitors of human neutrophil elastase

Drew Smith[1]*, Gary P Kirschenheuter[1], Josephine Charlton[1], David M Guidot[2] and John E Repine[2]

[1]NeXstar Pharmaceuticals, Inc., 2860 Wilderness Place, Boulder, CO 80301, USA and [2]Webb–Waring Institute for Biomedical Research and Department of Medicine at the University of Colorado Health Sciences Center, 4200 East 9th Avenue, Box C-321, Denver, CO 80262, USA

Introduction: We describe a new approach to drug discovery which joins the technologies of medicinal and combinatorial chemistry, allowing selection of the most active variant of a lead compound from a large ($>10^{12}$) pool. A small-molecule covalent inhibitor of elastase was coupled to a randomized pool of RNA, and this assembly was iteratively selected for oligonucleotide sequences that promote the covalent reaction of the inhibitor with the human neutrophil elastase (hNE) active site.
Results: Incorporation of the covalent inhibitor into the randomized pool increases the second-order rate of inactivation of hNE by ~15-fold; sequences selected from this pool show an additional ~20-fold increase in activity. The relative rate of cross-reaction with another serine protease, cathepsin G, was reduced >100-fold. Low doses of the inhibitor were found to prevent lung damage inflicted by human neutrophils in an isolated rat lung model of acute respiratory distress syndrome (ARDS).
Conclusions: This result supports the hypothesis that neutrophil elastase is a significant effector of inflammatory disease. More generally, our findings demonstrate that blending small molecules into combinatorial libraries is a feasible method of drug discovery.

Chemistry & Biology November 1995, **2**:741–750
Key words: acute respiratory distress syndrome, animal models, elastase, protease inhibitors, SELEX

Introduction

One of the dominant paradigms in drug discovery and development is that of medicinal chemistry, in which lead compounds are systematically altered by organic synthesis to optimize their pharmaceutical properties. Because each variant of the lead compound is the product of an individual synthetic sequence, only a few variants, usually less than 10^2, can be screened. Combinatorial chemistries are intended to accelerate drug discovery by the parallel screening or selection of 10^3 to 10^{15} candidates. These chemistries, however, require the coding, tagging or addressing of the candidates, a requirement that constrains the chemical and conformational space available to the starting libraries [1–3]. We describe an approach that seeks to access both the conformational space made available by combinatorial chemistry, and the range of chemical functions afforded by medicinal chemistry. Our scheme is outlined in Figure 1. A lead inhibitor compound is linked covalently to a DNA oligonucleotide, and this DNA 'splint' conjugate is then annealed to the fixed-sequence region of a randomized RNA pool. Using the iterative process of selection and amplification known as SELEX (Systematic Evolution of Ligands by EXponential enrichment) [4], those sequences that best promote the reaction of the lead compound with the target are isolated, a process that has been termed 'blended SELEX' [5]. In effect, the randomized RNA sequence pool provides $>10^{12}$ variants of the lead compound from which to select the optimal inhibitor. We chose elastase, a well characterized serine protease, as a target for blended SELEX.

Human neutrophil elastase (hNE) has been implicated circumstantially in several inflammatory diseases, including acute respiratory distress syndrome (ARDS), septic shock, myocardial ischemia-reperfusion injury, emphysema and arthritis [6–8]. The participation of neutrophils and neutrophil elastase is especially compelling in ARDS patients who have increased levels of neutrophils and oxidatively inactivated anti-proteases in their lungs [9].

Numerous elastase inhibitors, including irreversible inhibitors, which react with the active-site serine, have been described [10], and are potential lead compounds for blended SELEX. We chose a diphenyl phosphonate derivative of valine [11,12] as our lead compound. This class of inhibitors readily reacts with the elastase active site, but both the free inhibitor and the inhibitor–elastase conjugate are chemically stable under physiological conditions.

One of the advantages of SELEX as a drug discovery method is that selection conditions can be designed to emphasize desirable properties of the winning ligands. In this instance, we wished to obtain highly specific elastase inhibitors. Accordingly, we performed the selections at low concentrations of reactants ('k_{cat}/K_M conditions'), to emphasize specificity over reactivity. The

*Corresponding author.

 ISSN 1074-5521

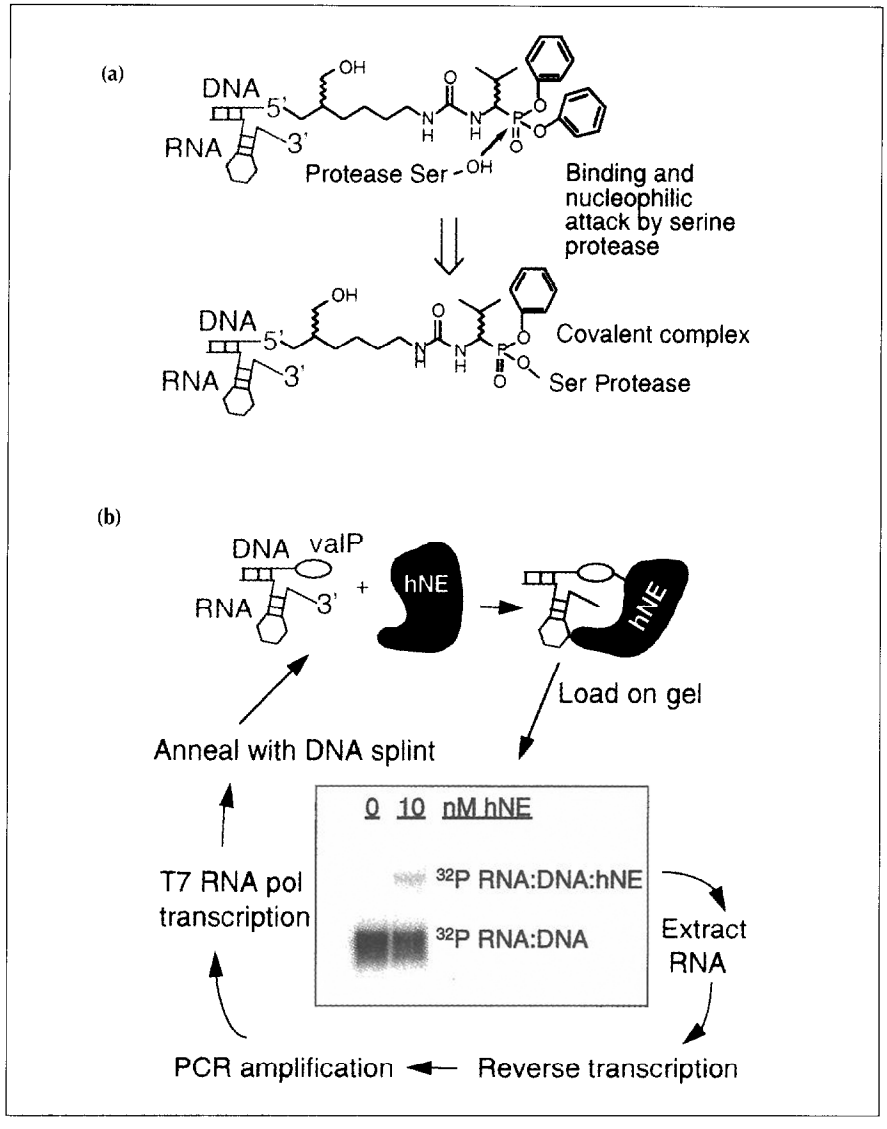

Fig. 1. 'Blended SELEX' selection scheme for hNE inhibitors. **(a)** Reaction with inhibitor. The valyl phosphonate moiety (valP) is shown conjugated to the 5' linker of the DNA splint oligonucleotide, which is in turn annealed to the SELEX RNA. Nucleophilic attack on the phosphorus center by the elastase active-site serine displaces a phenyl group, and results in a stable covalent complex between elastase and the DNA:valP splint. **(b)** Selection and amplification. The ^{32}P RNA:DNA:valP:hNE complexes were resolved from unreacted ^{32}P RNA:DNA:valP by electrophoresis through 4% polyacrylamide, TBE, 0.05 % SDS, and then recovered from the gel by the crush-and-soak method. This RNA was amplified by reverse transcription, PCR, and transcription by T7 RNA polymerase, essentially as described [24].

selected inhibitors have increased reactivity, but are much more specific than the valyl phosphonate lead compound, and do not cross-react detectably with other serine proteases.

One of the selected inhibitors was tested in an isolated perfused rat lung model of ARDS. The inhibitor proved highly potent and efficacious in preventing neutrophil-mediated lung weight gain. Because lung weight gain was completely suppressed with a highly specific elastase inhibitor, this result implicates hNE as an important mediator of lung damage in inflammatory disease.

Results and discussion

Using the template 40N7.1 (Fig. 2), we started with a pool of 100 pmol RNA transcribed from 10 pmol randomized DNA template. This DNA pool was composed of an average of 10 copies each of 6 x 10^{12} sequences. The RNA pyrimidine nucleotides are 2'-NH_2-substituted to enhance nuclease resistance [13].

The splint oligonucleotide is a synthetic DNA sequence that is complementary to the 5' fixed sequence of the SELEX RNA (Fig. 2), and is conjugated to the reactive valyl phosphonate moiety (valP) through an amino linker at its 5' end (Fig. 1). We refer to this conjugate as DNA:valP. This configuration places the reactive moiety physically near the randomized region of the SELEX RNA. A six-nucleotide 'dangling end' of arbitrary sequence was placed at the 5' end of the splint oligonucleotide; this allows the selection process to resolve the questions of what the length of the splint DNA–SELEX RNA double helix should be, and whether the bases near the reactive moiety should be paired or unpaired.

We selected inhibitors at low concentrations of reactants ('k_{cat}/K_M conditions'), so that both reactivity and binding affinity could contribute to selection. The concentration of hNE was 20 nM at the beginning of the selection, and reduced to 5 nM in the final rounds. The extent of the reaction was limited by keeping RNA in a 10- to 50-fold excess over hNE. Ten rounds of SELEX were performed according to the method outlined in Figure 1. The selection was stopped after no substantial increases in the second-order rate of inactivation were observed for three rounds (Fig. 3).

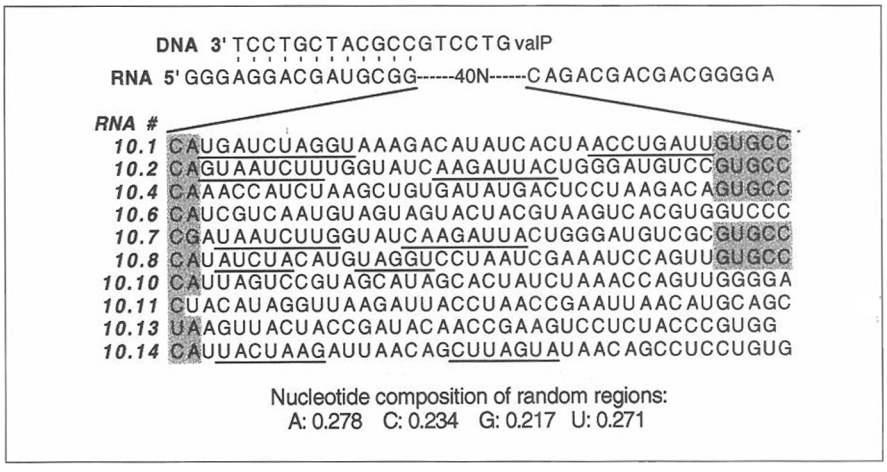

Fig. 2. Sample of selected sequences. The sequence of the DNA splint, and the fixed-sequence primer-binding regions of the RNA are shown at the top. Below are the sequences from the RNA random regions of the first 10 clones sequenced. Shaded areas indicate regions of sequence conservation. Underlines indicate the stems of potential RNA hairpins.

The sequences of 64 RNAs from the round-10 pool were determined. Twelve of these are clones, or 'pseudo-clones', of other sequences. Pseudo-clones are sequences that differ at only one or two positions from other sequences, and probably arise by errors in replication or transcription. Three features of these sequences are noteworthy (Fig. 2): (1) the mononucleotide composition of the randomized regions is not biased toward G (0.22 mol fraction G). PolyG binds and inhibits elastase *in vitro* [14] and a previous SELEX experiment yielded highly G-rich elastase ligands [13]. (2) Virtually all clones (61/64) extend the length of the splint helix by two or three base-pairs, usually with the sequence 'CA' or 'CAG'. (3) 23/64 clones share the sequence 'GUGCC' at the 3'-end of the random region. Because of the position of this sequence, we expect that it forms a structure with the 3' fixed-sequence region of the RNA.

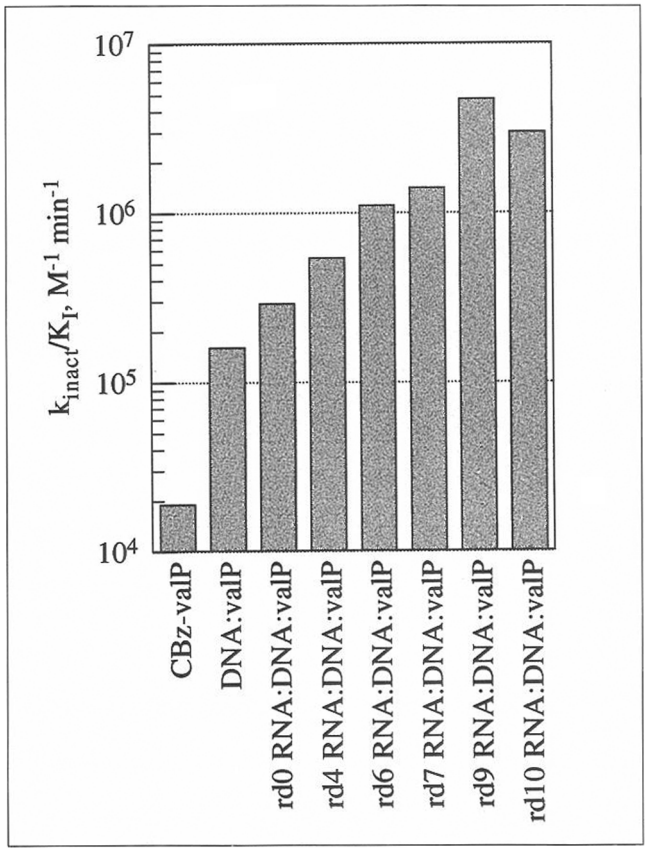

Fig. 3. The inactivation rate of hNE by selected inhibitory complexes increases over several rounds of selection. The second-order rate of inactivation of hNE was determined for the unconjugated valyl phosphonate (CBz-valP), the DNA splint (DNA:valP) and the DNA splint annealed to the pools of RNA from rounds 0–10 of SELEX, as described in Materials and methods.

Computer-assisted RNA folding studies [15] suggest a common structural motif. Thirty-nine of the cloned sequences were studied; about half (19/39) can form a perfect (i.e., without bulges or internal loops) hairpin at the 5' end of the random region. These potential hairpins are immediately 3' to the RNA–DNA splint helix, or are separated from the splint helix by a U nucleotide. The stems of the potential hairpins range in length from four to nine base-pairs, with seven base-pairs being the most common length, and there is no apparent sequence conservation in the stem. The loops of the hairpins range in size from four to seven bases, again with no apparent sequence conservation. The conserved positions of the hairpins suggest that they form a coaxial stack on the splint helix.

Inhibition of hNE

The selected assemblies proved to be potent hNE inhibitors. The inhibition of hNE activity (measured by hydrolysis of a chromogenic peptide substrate) by the RNA10.11:DNA:valP complex is shown in Figure 4a. Two parameters are measured in this assay: v_0, the initial, rapid equilibrium rate of peptide hydrolysis, and $k_{obs\ inact}$, the observed rate of enzyme inactivation. Second-order rate constants for inactivation (k_{inact}/K_I), derived from linear regression of the plots of $k_{obs\ inact}$ versus inhibitor concentration (Fig. 4b) are given in Table 1. Comparisons of this parameter show that the selected RNAs increase the activity of the valyl phosphonate more than two orders of magnitude as compared to the free inhibitor, from 10^4 to $>10^6$ M^{-1} min^{-1}. Coupling of the valyl phosphonate to the DNA oligonucleotide, and complexing this conjugate to random RNA also increases inactivation activity. These increases may result from the affinity of hNE, which is positively charged at

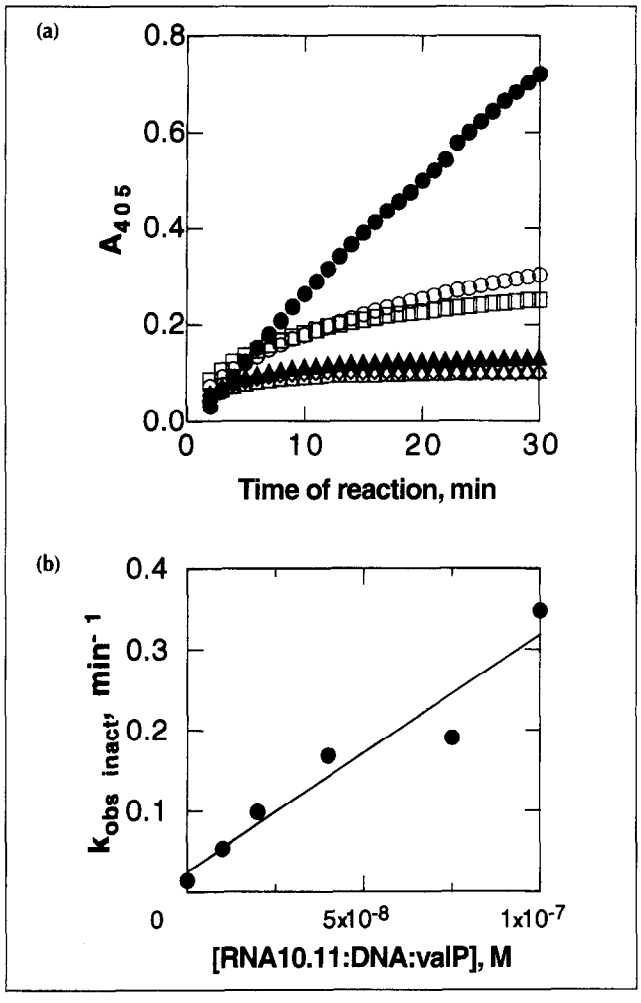

Fig. 4. RNA10.11:DNA:valP is a potent inhibitor of hNE activity. **(a)** hNE activity assay. The assay measures the increase in the absorbance at 405 nm (A_{405}) as hNE cleaves a test substrate. RNA10.11:DNA:valP concentrations: ● 0 nM; ○ 10 nM, □ 20 nM; ▲ 40 nM; △ 75 nM; ◇ 100 nM. **(b)** Replot of inactivation rate versus inhibitor concentration. The slope of the linear regression through the replot of $k_{obs\ inact}$ versus RNA:DNA:valP concentration yields the apparent second-order rate constant for inhibition, $\frac{k_{inact\ app}}{K_I}$.

neutral pH, for nucleic acids, which are negatively charged. The increase in k_{inact}/K_I for the selected ligands over that of the starting pool is not large, 10- to 20-fold; most SELEX experiments increase binding affinities by two to three orders of magnitude [5]. The weakness of the response to selection may reflect the constraint that the RNA bind near the active site of hNE, rather than being allowed to find the optimal binding site.

A complementary assay measures the extent of coupling of the DNA:valP conjugate to hNE by gel retardation of radioactively labeled splint DNA (Fig. 5a). The stability of this coupling under the gel conditions (7 M urea, 0.05 % SDS, 45–50 °C) indicates that the inhibitor forms a covalent bond with hNE. The time course of the reaction shows apparent first-order kinetics, but the extent of the reaction is limited to 0.3–0.45 of the total DNA:valP, depending on the batch of DNA:valP. Because we do not observe any loss of coupling after extended incubation, we do not attribute incomplete coupling to reversal of the inhibitor–hNE bond. Instead, we propose that only one stereoisomer of the inhibitor, which is a racemic mixture, reacts to a significant extent with hNE. In this case a limit of half of the total DNA:valP reacted is expected if the two stereoisomers are present in equal amount and only one is active. Alternatively, hNE could react nonproductively with the inhibitor, degrading it without forming a covalent bond.

When the gel assay is performed at hNE excess, so that there is no competition with a peptide substrate, or between active and inactive stereoisomers of the inhibitor, saturation kinetics are observed (Fig. 5b). Michaelian constants for the covalent reaction are given in Table 1. The second-order rate constants for this assay ($2–5 \times 10^7\ M^{-1}\ min^{-1}$) are ~10-fold higher than those in the peptide hydrolysis assay ($2–5 \times 10^6\ M^{-1}\ min^{-1}$). Part of this difference can be attributed to correction in the gel assay for the fraction of inhibitor that is active, while part may be a consequence of the absence of competition by inactive complexes for hNE.

Table 1. Rate and binding constants of inhibitors.

Inhibitor	k_{inact}/K_I[a] ($M^{-1}\ min^{-1}$)	K_I(M)[b]	k_{cat} (min^{-1})[c]	K_M (M)[c]	k_{cat}/K_M[c] ($M^{-1}\ min^{-1}$)
CBz–valP	$1.9\ (\pm0.5) \times 10^4$	nd	nd	nd	nd
DNA:valP	$1.6\ (\pm0.3) \times 10^5$	$>10^{-6}$	nd	nd	$3.3\ (\pm0.5) \times 10^5$
RNA40N7.1:DNA:valP[d]	$2.9\ (\pm0.1) \times 10^5$	$>10^{-7}$ [b]	0.38 (± 0.09)	$1.3\ (\pm0.6) \times 10^{-7}$	$2.9\ (\pm1.4) \times 10^6$
RNA10.2:DNA:valP	$5.6\ (\pm0.6) \times 10^6$	$4\ (\pm5) \times 10^{-8}$ [b]	3.6 (± 0.6)	$1.7\ (\pm0.4) \times 10^{-7}$	$2.1\ (\pm0.7) \times 10^7$
RNA10.6:DNA:valP	$5.7\ (\pm2.2) \times 10^6$	$2\ (\pm2) \times 10^{-8}$ [b]	3.0 (± 1.2)	$1.3\ (\pm1.0) \times 10^{-7}$	$2.3\ (\pm2.1) \times 10^7$
RNA10.11:DNA:valP	$2.4\ (\pm0.3) \times 10^6$	$5\ (\pm6) \times 10^{-9}$ [b]	3.4 (± 0.6)	$7.1\ (\pm0.4) \times 10^{-8}$	$4.8\ (\pm0.9) \times 10^7$

Numbers are the mean (± standard error). 'nd', not done.
[a]Enzymatic assay, second-order rate constant for irreversible inactivation.
[b]Enzymatic assay, reversible competitive inhibition, using the peptide hydrolysis assay for elastase.
[c]Gel retardation assay, rate constants for covalent complex formation.
[d]Random RNAs from the starting pool conjugated to DNA:valP.

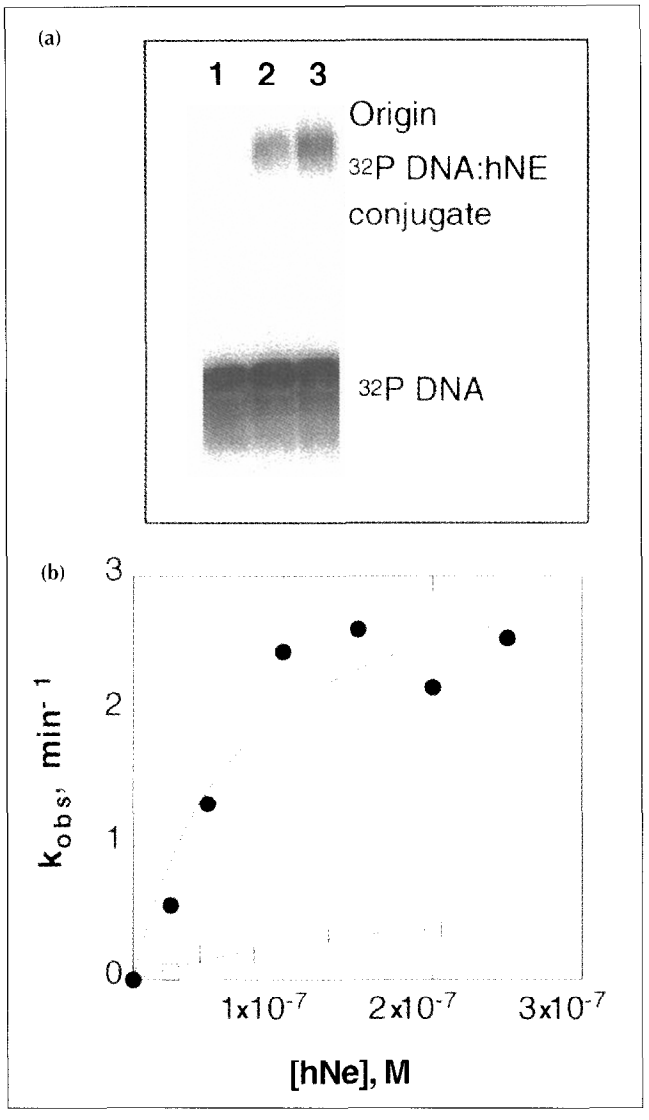

Fig. 5. Michaelian rate constants can be determined for the covalent reaction of DNA:valP with hNE. **(a)** Reaction of splint with hNE. Lane 1, no hNE control; Lane 2, 10 nM hNE reacted for 10 s; Lane 3, 10 nM hNE reacted for 20 s. **(b)** Evaluation of rate constants. Values of k_{obs} for each concentration of hNE were replotted and fitted to the Michaelis–Menten equation for the starting RNA pool (RNA40N7.1; ❒) and for an inhibitor selected after 10 rounds of SELEX (RNA10.11; ●).

Comparison of k_{cat} values of selected clones with those of the starting pool (Table 1) shows that selection acted to increase k_{cat} by a factor of 5- to 10-fold. Because the inhibitor reacts with hNE to form a dead-end complex, k_{cat} must represent a step at or before covalent bond formation. The selection therefore must have served to increase the rate of one or more of these steps. K_M values were not significantly reduced by the selection, which might indicate that binding affinity to hNE was not increased. Increases in the rate of covalent bond formation could cause increases in K_M that would mask tighter binding by the selected RNAs, however. Analysis of reversible binding and inhibition (below) indicate that selected ligands do exhibit increased affinity for hNE.

Non-covalent competitive inhibition

The selected assemblies are competitive inhibitors of hNE. The parameter for the initial velocity of peptide hydrolysis, v_0, can be used to evaluate rapid equilibrium reversible inhibition of hNE by the RNA:DNA:valP complexes. We determined the values of the Michaelian parameters $V_{max\ app}$ and $K_{M\ app}$ for peptide hydrolysis at a series of inhibitor concentrations (Fig. 6). The apparent peptide K_M is increased by the inhibitor, whereas there is no significant effect on apparent peptide V_{max}, behavior that is consistent with fully competitive inhibition. No significant effects on V_{max} or K_M were observed for the random RNA40N7.1:DNA:valP complex, or for the DNA:valP conjugate alone. K_i values for reversible inhibition are reported in Table 1. These values, which should correspond to the equilibrium dissociation constants of the inhibitors, are of the order of 10^{-8} M.

Specificity

We selected hNE inhibitors under k_{cat}/K_M conditions with the expectation that the winning ligands would show high specificity for hNE. We tested this expectation by determining cross-reactivity with cathepsin G, a serine protease that has substrate specificity similar to hNE, and, like hNE, is positively charged at neutral pH. Figure 7 compares inactivation of hNE or cathepsin G by free valyl phosphonate or selected RNA:DNA:valP inhibitors. The second-order rate constant for inactivation by free valyl phosphonate is only four-fold less for cathepsin G than for hNE. In contrast, inactivation of cathepsin G by the RNA:DNA:valP complexes is undetectable, and is at least 400-fold less than the rate of inactivation of hNE. The SELEX process has therefore acted to potentiate the reaction of the valyl phosphonate moiety with hNE at low concentrations in a specific manner, without making it generally more reactive. Although our inhibitors do not inactivate cathepsin G, they do display reversible partial inhibition at high con-

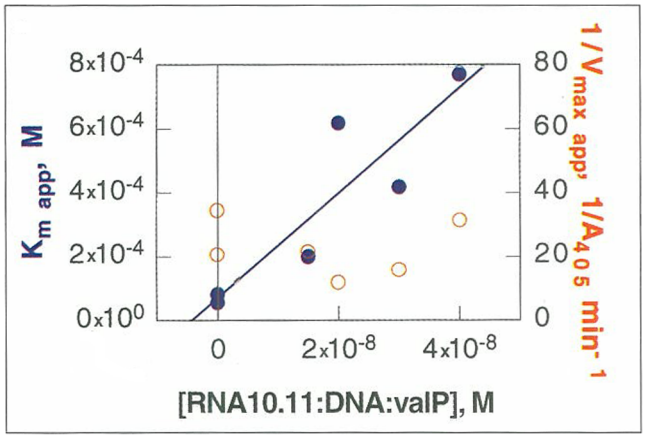

Fig. 6. Reversible, competitive inhibition by RNA:DNA:valP assemblies. Apparent K_M (●) and $1/V_{max}$ (○) values for the elastase peptide substrate in the presence of RNA10.11:DNA:valP are shown. The x intercept of a linear regression of $K_{M\ app}$ versus inhibitor concentration yields the negative of the K_i value for reversible competitive inhibition (Table 1).

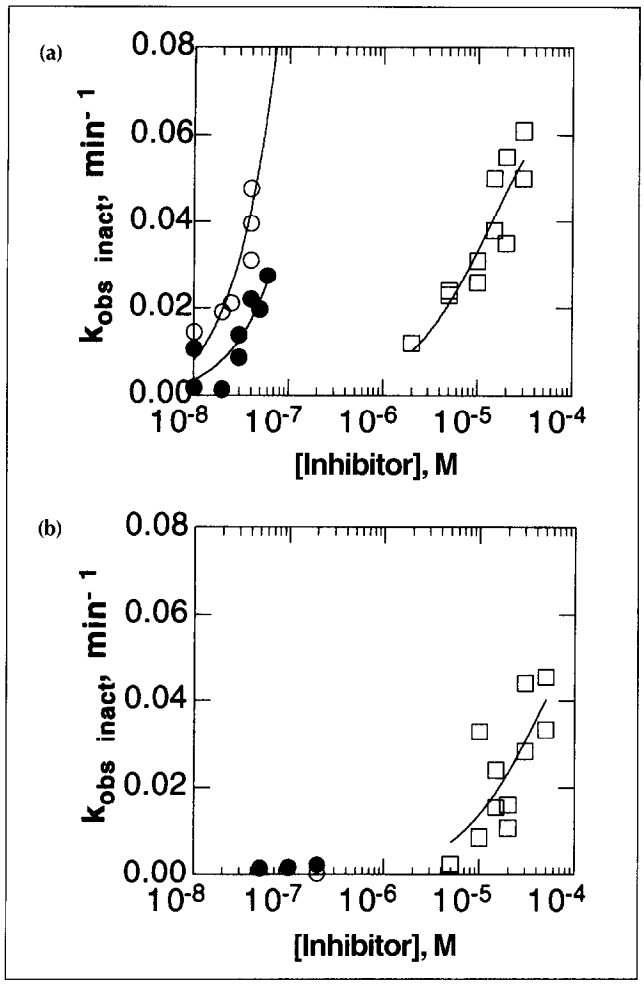

Fig. 7. RNA:DNA:valP complexes specifically inhibit hNE activity. ○ RNA10.2:DNA:valP; ● RNA10.14:DNA:valP; □ CBz-valP. **(a)** hNE inactivation. Assays were performed as described in Materials and methods. **(b)** Cathepsin G inactivation. Assays and analysis similar to those described for hNE were performed for cathepsin G. Cathepsin G (Calbiochem) was at 40nM, and its substrate (*N*-methoxysuccinyl Ala-Ala-Pro-Phe *p*-nitroanilide, Calbiochem) was at 0.2 mM.

centrations. Thrombin, another serine protease, is also not inactivated by our inhibitors (data not shown).

Structural basis of hNE–RNA interaction

Elastase is a highly positively charged protein at physiological pH, and is likely to associate with polyanions such as RNA through favorable ionic interactions. Polyguanylic acid inhibits hNE, possibly by a competitive mechanism, and this inhibition is salt-sensitive [14]. Salmon sperm DNA appears to be a partial non-competitive inhibitor, and also shows salt-sensitivity [16]. Irreversible inhibition by selected RNA:DNA:valP assemblies is also highly salt-sensitive (Fig. 8), with the rate of inactivation reduced to background levels at ≤200 mM total Na^+. The SELEX-derived ligands reported here therefore share salt-sensitivity with the non-specific nucleic acids, suggesting that all of these nucleic acids bind to hNE through favorable ionic interactions. Elastase has a patch or band of arginine residues [17], constituting a likely binding site for nucleic acids.

Given the general ability of nucleic acids to bind to and inhibit hNE, one may ask whether the RNA sequences were selected merely on the basis of their ability to associate stably with the DNA:valP splint. Figure 9 shows thermal melting data for complexes between the DNA:valP splint and either unselected RNA, or RNA10.11. Two observations can be made concerning this data. First, the T_m of the RNA40N7.1:DNA:valP helix (50 °C) is well above the temperature at which selections were done (37 °C). Since the equilibrium between melting and annealing shifts towards annealing by a factor of 10 for every 3 °C below the T_m, only a tiny fraction of the starting pool was not annealed to the DNA:valP oligonucleotide. It is therefore unlikely that sequences were selected for their more stable association between the RNA and the DNA:valP oligonucleotide. Second, a substantial (4–7 °C) increase in T_m may be due to the 5' CA sequence which extends the helix by two base pairs (Fig. 2). Because this sequence confers only an incremental increase in stability at the experimental temperature, it was probably selected through its effects on the stereochemistry of the complex, for instance, by shortening the six-base 'dangling end' to four bases (Fig. 2).

Truncation experiments, in which portions of the 3' end were removed, show that sequences distant from the RNA10.2–DNA:valP double helix are required for full activity (Table 2). The smallest truncation, which removes the 3'-terminal 16 nucleotides of RNA10.2, causes a four-fold loss in the second-order rate of inactivation. Additional truncations, down to 42 nucleotides, cause only incremental additional losses of inhibitory activity. Comparable results were obtained for

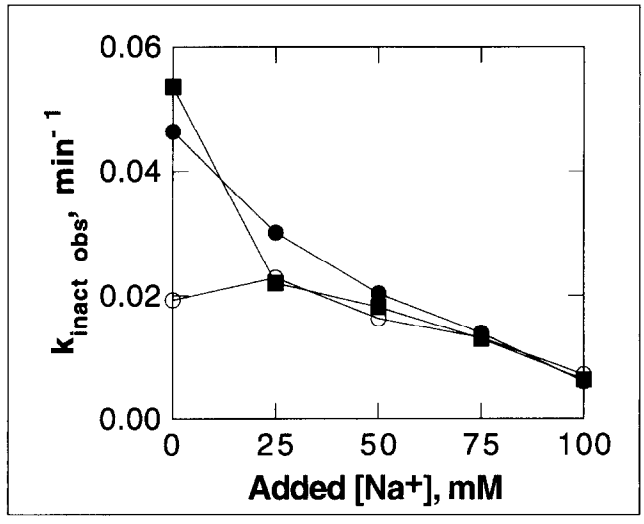

Fig. 8. Irreversible inhibition of hNE by selected RNA:DNA:valP complexes is highly salt-sensitive. ○ No inhibitor; ■ RNA10.6:DNA:valP; ● RNA10.11:DNA:valP. Elastase inhibition assays were performed as described in Materials and methods, and in the legend to Figure 4. The concentration of RNA:DNA:valP assemblies was 50 nM. The amount of Na^+ added to Hank's balanced salt solution (HBSS) is indicated on the x-axis; HBSS is 137 mM Na^+, 5 mM K^+.

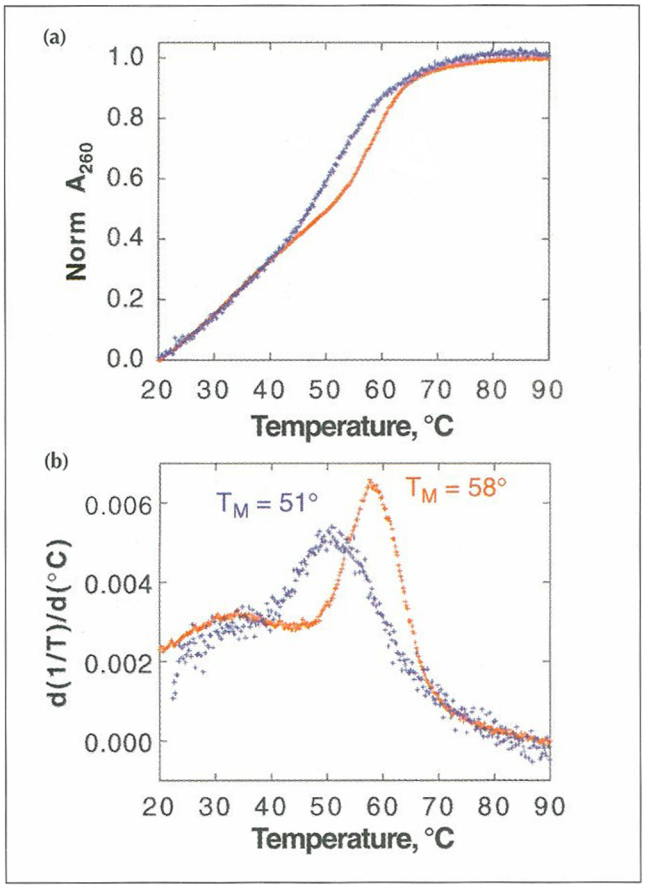

Fig. 9. The RNA:DNA:valP double helix is stable at the experimental temperature. Melting curves of RNA:DNA:valP complexes are shown. **(a)** Normalized absorbance curves. Red, RNA10.11; blue, RNA40N7.1. **(b)** Determination of T_m values. Data from (a) were replotted as the first derivative of (transmittance)$^{-1}$ with respect to temperature. The peaks of these plots correspond to the T_m values [28]. Assignment of the sharper peaks at 51 °C (RNA40N7.1, blue), and 58 °C (RNA10.11, red) to the RNA–DNA:valP double helices was made by titrating in increasing amounts of the DNA:valP oligonucleotide.

RNA10.11 (Table 2). These results indicate that structures important for inhibitory activity are distributed throughout the selected RNA sequences.

Inhibition of tissue damage by human neutrophils

Human neutrophil elastase is implicated in a number of inflammatory diseases; highly specific and potent inhibitors are useful in clarifying the role of hNE in disease. We used an *ex vivo* perfused rat lung system to test the ability of the inhibitors to protect lungs from interleukin-1 (IL-1) induced, human neutrophil-mediated damage. Large accumulations of neutrophils are found in lung lavages of ARDS patients, and are strongly implicated in the pathogenesis of ARDS [18,19]. IL-1 is also found at elevated levels in lung lavages of ARDS patients, and induces neutrophil accumulation and lung leak in rats [20].

In the rat lung model, 10^6 human neutrophils are circulated through isolated, ventilated lungs in 30 ml of buffered perfusate, and an ARDS-like inflammatory response is induced by intra-tracheal administration of IL-1 [21,22]. The resulting inflammatory response perturbs lung tissue, leading to edema-like weight gain (Fig. 10, expt 1 vs 2), which is measured after one hour. Adding 20 pmol (0.5 μg) of the RNA10.11:DNA:valP assembly to the perfusate before IL-1 administration decreases neutrophil-mediated weight gain (Fig. 10, expt 4). The reduction in lung weight gain compared to a positive control is highly significant (Fig. 10, expt 1 vs 4, $P<0.001$) using the Student–Newman–Keuls multiple comparison test; weight gain is not significantly greater than the negative control (Fig. 10, expt 2 vs 4, $P>0.05$). Adding only the RNA10.11:DNA:valP assembly to the system does not cause lung weight gain (Fig. 10, expt 3).

Control experiments show that the protective effect is mediated primarily by hNE inactivation; RNA10.11 without the DNA:valP splint, which is not expected to inhibit hNE at the low concentration used, does not reduce lung weight gain (Fig. 10, expt 5 (expt 3 vs 5, $P<0.001$)). Similarly, the DNA:valP splint alone is not effective (Fig. 10, expt 6 (expt 3 vs 6, $P<0.001$)). *In vitro* experiments with the full RNA10.11:DNA:valP assembly show that neutrophil viability, chemotaxis, and superoxide production are unaffected by the inhibitor (data not shown). These results suggest that highly specific and potent irreversible inhibitors of hNE have therapeutic potential in the treatment of ARDS, and possibly in other neutrophil-mediated inflammatory diseases.

Table 2. Effects of 3' truncations on hNE inactivation.

RNA	RNA length/3' nt removed	$k_{inact\ app}/K_I$, $M^{-1}\ min^{-1}$
10.2	71/0	5.6×10^6
10.2.55	55/16	1.4×10^6
10.2.47	47/24	1.2×10^6
10.2.42	42/29	1.0×10^6
10.11	71/0	2.4×10^6
10.11.49	49/22	9.2×10^5
10.11.40	40/31	5.9×10^5

The indicated RNA sequences were annealed to the DNA:valP splint, and hNE inactivation assays were performed as described in Materials and methods. Truncated RNAs were produced by using synthetic DNA oligonucleotides whose 5' ends correspond to the desired 3' terminus as PCR primers on the full-length template. Double-stranded DNA products of the appropriate length were purified by gel electrophoresis, and used as templates for transcription. nt, nucleotides.

Significance

The blending of combinatorial and medicinal chemistries is a drug discovery strategy aimed at fusing the strengths of both approaches. Medicinal chemistry requires a large amount of labor to screen a relatively small number of compounds. Combinatorial chemistry selects from a large number of compounds, but usually only on the basis of affinity to a target, without reference to desirable functional properties

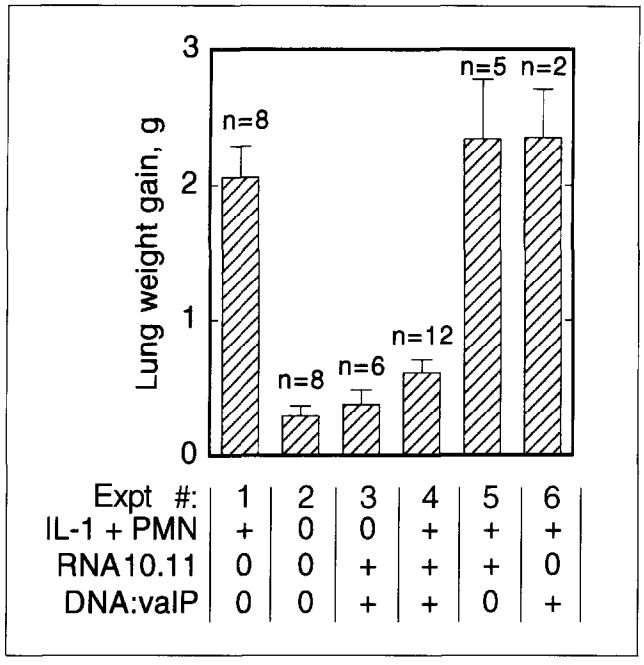

Fig. 10. The RNA10.11:DNA:valP complex has a protective effect in the human neutrophil-perfused rat lung model of ARDS. 10^6 PMN (neutrophils), and 20 pmol of each nucleic acid were used in each experiment. Bars show the mean of n experiments, error bars indicate one standard error. The level of significance in comparison to the positive control using the Student–Newman–Keuls multiple comparison test is $P < 0.001$ for experiments 2, 3 and 4; not significant for 5 and 6.

[1–5]. The incorporation of a functional moiety into a combinatorial library greatly increases the likelihood that the winning sequences will have desirable properties. Conversely, one can think of this blended approach as a method to obtain highly active and highly specific variants of a small molecule. The ability to 'build-in' a desirable function is a feature that distinguishes SELEX from strategies such as phage display or generation of monoclonal antibodies. The blending of medicinal and combinatorial chemistries is a general strategy in drug discovery and development, which can be applied to a wide range of small molecules and libraries, accelerating the search for compounds that will advance disease treatment.

These principles are demonstrated by the elastase inhibitors generated through blended SELEX; the inhibitors are much more potent and specific than the valyl phosphonate moiety alone. These inhibitors are shown to be highly efficacious at low doses in an isolated, perfused rat lung model of ARDS. A dose of 0.5 μg in 30 ml of perfusate is sufficient to abolish neutrophil-mediated lung weight gain, without affecting neutrophil viability, motility or adherence.

Finally, we note that the blended SELEX strategy may be applied to other fields, such as the investigation of RNA-based catalysis. In particular, the suggestion that modified nucleotides acted as catalytic cofactors in an RNA world [23] might be fruitfully studied using a blended SELEX approach.

Materials and methods

Synthesis of the co-ligand for human neutrophil elastase

The diphenylphosphonovaline co-ligand **3** may be synthesized from the known benzyl carbamate-protected diphenylphosphonovaline **1** as outlined in Figure 11. Condensation of isobutyraldehyde, benzyl carbamate (Cbz) and triphenylphosphite gave compound **1** in 55% yield. The Cbz group was removed with 30% HBr/AcOH and the resulting HBr salt converted to the free amine **2** in 86% overall yield. Treatment of compound **2** with *N,N'*-disuccinimidyl carbonate (DSC) in acetonitrile provides the desired co-ligand **3** which may be conjugated to the amino-DNA splint via the *N*-hydroxy succinimide (NHS) ester moiety.

Synthesis of N*-benzyloxycarbonyl-O,O'- diphenyl-phosphono-valine (compound 1)*

Benzyl carbamate (30.23 g, 0.20 mol), isobutyraldehyde (27.25 ml, 0.30 mol) and triphenylphosphite (52.4 ml, 0.20 mol) were dissolved in 30 ml of glacial acetic acid in a 250 ml round-bottom flask. After stirring at room temperature for 5 min, the solution was heated to 80–85 °C in an oil bath for 3 h. The

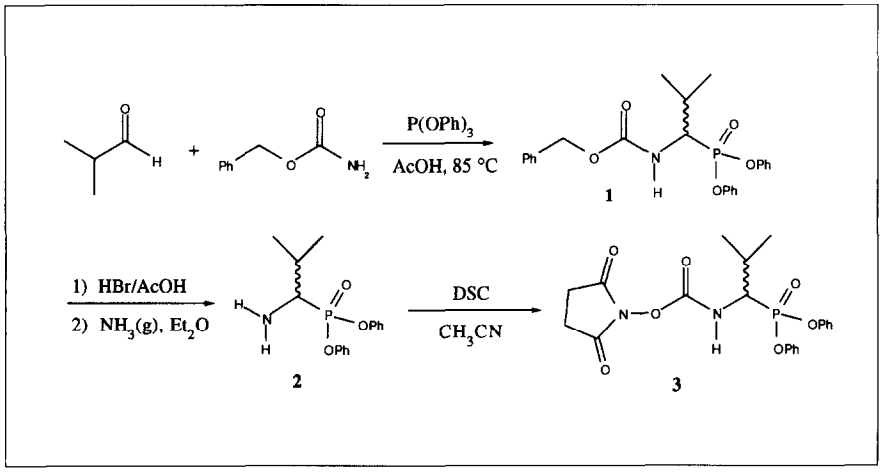

Fig. 11. Scheme for synthesis of inhibitor. For details see Materials and methods.

mixture was concentrated to an oil on a rotary evaporator equipped with a vacuum pump and using a bath temperature of 90–95 °C. The oil was subsequently dissolved in 250 ml of boiling methanol, filtered and chilled to −15 °C to promote crystallization. The crystalline solid was filtered, washed with cold methanol, air dried and then dried overnight in a vacuum desiccator to give 48.2 g (55%) of the product.

*Synthesis of O,O'-diphenylphosphonovaline (compound **2**)*

N-Benzyloxy-carbonyl-*O,O'*-diphenylhosphonovaline (21.97 g, 50.0 mmol) was treated with 18 ml of 30% HBr/HOAc. After 1 h, the solidified reaction mixture was suspended in 25 ml of glacial acetic acid and concentrated to an orange solid. The solid was triturated with 50 ml of ether overnight, filtered and washed with ether until off-white. A total of 17.5 g (91%) of the HBr salt was obtained. This salt was suspended in 150 ml of ether and gaseous ammonia bubbled through the suspension for 15 min. The ammonium bromide was filtered off and washed with ether. The filtrate was concentrated and the solid residue dried under vacuum to give 13.05 g (86% overall) of the desired free amine **2**.

*Synthesis of N-succinimidyloxycarbonyl-O,O'-diphenylphosphonovaline (compound **3**)*

N,N'-Disuccinimidyl carbonate (243 mg, 0.95 mmol) was dissolved in 5 ml of dry acetonitrile. A solution of *O,O'*-diphenylphosphonovaline (289 mg, 0.95 mmol) in 5 ml of dry acetonitrile was added and the mixture stirred at room temperature for 2 h. The precipitated product was filtered, washed with dry acetonitrile and dried under vacuum to give 229 mg (54%) of a white solid.

Coupling of valyl phosphonate diphenyl ester to splint DNA

The splint DNA is a synthetic oligonucleotide (sequence shown in Fig. 3) that contains a hexylamine (2-methyl hydroxyl) linker at the 5' phosphate (Operon). To couple the valyl phosphonate diphenyl ester to the splint DNA, 200 nmol of DNA was dissolved in 500 µl DMSO plus 50 µl 0.5 M $NaBO_3$, pH 9.0, and then added to 5.2 mg of the NHS ester of the valyl phosphonate, **3**, allowed to react at room temperature for 1 h, then ethanol precipitated. The oligonucleotide was resuspended in 200 µl of H_2O, then purified by reverse-phase HPLC in a gradient of acetonitrile:triethylamine acetate.

SELEX

For the hNE reaction, 20–100 pmol SELEX RNA at a concentration of 1 µM was annealed to a 1.1-fold excess of splint DNA:valP by heating to 65 °C and cooling slowly to 35 °C. The reaction was initiated by adding hNE to a final concentration of 5–20 nM, at a 5- to 20-fold excess of RNA over hNE. After incubation for 5–10 min at 37 °C, the reaction was quenched by adding SDS to 0.1%.

The ^{32}P RNA:DNA:valP:hNE complexes were resolved from unreacted ^{32}P RNA:DNA:valP by electrophoresis through a 4% polyacrylamide gel containing TBE and 0.05% SDS, and then recovered from the gel by the crush-and-soak method. This RNA was amplified by reverse transcription, PCR and transcription by T7 RNA polymerase, essentially as described [24].

Individual sequences were cloned by blunt-end ligation of PCR DNA into vector 'PCR-script SK+' (Stratagene), and transformation into 'Epicurian Competent SURE Cells' (Stratagene). DNA sequences were obtained by enzymatic sequencing.

Elastase activity and inhibition assays

Elastase substrate (*N*-methoxysuccinyl Ala-Ala-Pro-Val *p*-nitroanilide, AAPV-pNA, Calbiochem) at 0.2 or 0.3 mM was mixed with inhibitor at the indicated concentration in 0.2 ml Hank's balanced salt solution (HBSS), 25 mM Tris, pH 7.5, 0.01% human serum albumin, in a microtiter plate well at 37 °C. The reaction was initiated by adding hNE (Calbiochem), and absorbance at 405 nm was monitored in a BioTek EL312 microtiter plate reader. The data were fit (Kaleidagraph, Synergy Software) to the following equation:

$$A_{405} = v_0 \frac{\left(1 - e^{[-k_{obs\ inact}t]}\right)}{k_{obs\ inact}} + A_t$$

where v_0 is the initial rate of peptide hydrolysis, $k_{obs\ inact}$ is the observed rate of inactivation, and A_t is a displacement factor. This equation describes the behavior of an inhibitor that initially binds to the enzyme reversibly to attain a rapid equilibrium, and subsequently reacts with first-order kinetics to inactivate the enzyme [25,26]. The rapid equilibrium assumption was tested by continuous monitoring of the colorigenic reaction of hNE with AAPV-NA. When 50 nM of the RNA10.11:DNA:valP complex was added to an ongoing reaction, the slope of the A_{405} versus time plot was deflected instantly, within the limits of detection (<5 s, data not shown).

The apparent second-order rate constant of inactivation, $\frac{k_{inact\ app}}{K_I}$ was obtained by replotting $k_{obs\ inact}$ as a function of inhibitor concentration, and determining the slope of the least-squares linear regression. To correct for competition between elastase substrate and inhibitor, the true second-order rate of inactivation was calculated using a model of full competitive inhibition [27]:

$$\frac{k_{inact}}{K_I} = \frac{k_{inact}}{K_I}\ app \left(1 + \frac{[AAPV - pNA]}{K_{M\ AAPV-pNA}}\right)$$

The value used for $K_{M\ AAPV-pNA}$ is 100 mM. Salt-sensitivity experiments were performed in HBSS, 25 mM Tris, pH 7.5, 0.01% human serum albumin, with 0–100 mM NaCl added.

Covalent reaction with hNE

Splint DNA:valP was radiolabeled at the 3' end with ^{32}P cordycepin (New England Nuclear) and terminal deoxynucleotide transferase (Promega), and then annealed with RNA in HBSS, 25 mM Tris, pH 7.5. The reaction was initiated by adding a ≥3-fold excess of hNE at a series of concentrations at 37 °C. Two to five aliquots were withdrawn at a range of time points, and quenched with two volumes of 10 M urea, 1% SDS. Reaction extent was limited to ≤20% of the total DNA. ^{32}P DNA:valP:hNE complexes were resolved from free ^{32}P DNA:valP by electrophoresis through 10% polyacrylamide gels with 7 M urea, 0.05% SDS. The relative amount of ^{32}P DNA:valP conjugated to hNE was quantified using a Fujix BAS1000 Phosphorimager.

The apparent first-order rate constant, k_{obs}, was determined from the slope of a plot of $\ln(S_t/S_0)$ versus time, where S_t is the amount of unreacted ^{32}P splint DNA:valP remaining at a given time, and S_0 is the initial amount, corrected for the fraction of active compound, determined by extended reactions. The value of k_{obs} was replotted as a function of hNE concentration, and fitted to the Michaelis–Menten equation to obtain k_{cat} and K_M for the covalent reaction of the splint DNA:valP with hNE.

Thermal melts

The buffer used for thermal melting experiments was HBSS supplemented with 20 mM HEPES, pH 7.5, purged with He gas and filtered. Measurements were made in a temperature-controlled Cary 1E UV–Vis spectrophotometer. RNA (typically 12 μg) and DNA:valP were added to 2.4 ml of buffer which was then pre-melted by heating from 5 °C to 95 °C at a rate of 12 °C min^{-1}, then cooled to 5 °C and held. Melting curves were obtained by heating from 5 °C to 95 °C at a rate of 1 °C min^{-1}. The absorbance at 260 nm was recorded at 0.2 min intervals. Repeated melting curves on the same sample showed no evidence of hysteresis.

Isolation and perfusion of lungs

After Sprague–Dawley adult male rats (350 ± 50 g) were anesthetized with pentobarbital (60 mg kg^{-1}, i.p.), a tracheotomy cannula was placed and secured with 2-O ligature. Lungs were ventilated with a tidal volume of 3 cc at a rate of 60 min^{-1} with a gas mixture containing 5% CO_2, 21% O_2 and 74% N_2. Following midline thoractomy, a 4-O ligature was loosely placed around the root of the pulmonary outflow tract. Heparin (200 units) was then injected into the right ventricle and allowed to recirculate. A rigid cannula was subsequently placed into the right ventricle, threaded into the pulmonary outflow tract, and secured with the ligature. The left ventricle was incised next and a drainage cannula was inserted and secured with a 2-O ligature. Lungs and heart were excised, placed in an isolated lung chamber, and ventilated with 2.5 cm of positive-end expiatory pressure. Lungs were perfused free of blood using Earle's balanced salt solution (Sigma Chemical Co.) containing (g l^{-1}) 0.265 calcium chloride, 0.098 magnesium sulfate, 0.4 potassium chloride, 6.8 sodium chloride, 0.122 sodium phosphate monobasic, and 1 D-glucose to which was added 2.2 g l^{-1} sodium bicarbonate and 40 g l^{-1} Ficoll-70 (Sigma Chemical Co.), and the final pH adjusted to 7.40. Perfusate (30 ml) was passed through the lungs to remove residual blood. The system was then closed and 30 ml of perfusate was continuously recirculated at a rate of 40 ml kg^{-1} body weight min^{-1}. Pulmonary artery pressures were continuously monitored with a pressure transducer and weight increases were monitored with a force transducer. A 20-min equilibration period was followed by a 60 min experimental protocol.

Purification of human neutrophils

Heparinized blood was obtained from healthy volunteers. Neutrophils were isolated using a Percoll gradient and differential centrifugation. Each preparation contained highly purified (>99 %) neutrophils which were suspended in HBSS at a concentration of 2×10^7 ml^{-1}.

Acknowledgements: We thank J. Reed for skillful assistance with HPLC purification, and B. Polisky and L. Gold for critical reading of the manuscript.

References

1. Kenan, D., Tsa, D. & Keene, J. (1994). Exploring molecular diversity with combinatorial shape libraries. *Trends Biochem. Sci.* **19**, 57–64.
2. Freier, S., Konings, D., Wyatt, J. & Ecker, D. (1995). Deconvolution of combinatorial libraries for drug discovery: a model system. *J. Med. Chem.* **38**, 344–352.
3. Janda, K. (1994). Tagged versus untagged libraries: methods for the generation and screening of combinatorial chemical libraries. *Proc. Natl. Acad. Sci. USA* **91**, 10779–10785.
4. Gold, L. (1995). Oligonucleotides as research, diagnostic, and therapeutic agents. *J. Biol. Chem.* **270**, 13581–13584.
5. Gold, L., Polisky, B., Uhlenbeck, O. & Yarus, M. (1995). Diversity of oligonucleotide functions. *Annu. Rev. Biochem.* **64**, 763–797.
6. Powers, J., *et al.*, & Kam, C. (1993). Proteases — structures, mechanism and inhibitors. *Agents Actions Suppl.* **42**, 3–18.
7. Jochum, M., Machleidt, W. & Fritz, H. (1993). Proteolysis-induced pathomechanisms in acute inflammation and related therapeutic approaches. *Agents Actions Suppl.* **42**, 51–69.
8. Doring, G. (1994). The role of neutrophil elastase in chronic inflammation. *Am. J. Respir. Crit. Care Med.* **150**, S114–S117.
9. Repine, J. (1992). Scientific perspectives on adult respiratory distress syndrome. *Lancet* **339**, 466–469.
10. Edwards, P. & Bernstein, P. (1994). Synthetic inhibitors of elastase. *Med. Res. Rev.* **14**, 127–194.
11. Oleksyszyn, J. & Powers, J. (1989). Irreversible inhibition of serine proteases by peptidyl derivatives of alpha-aminoalkylphosphonate diphenyl esters. *Biochem. Biophys. Res. Commun.* **161**, 143–149.
12. Oleksyszyn, J. & Powers, J. (1991). Irreversible inhibition of serine proteases by peptide derivatives of (alpha-aminoalkyl)phosphonate diphenyl esters. *Biochemistry* **30**, 485–493.
13. Lin, Y., Qiu, Q., Gill, S. & Jayasena, S. (1994). Modified RNA sequence pools for *in vitro* selection. *Nucleic Acids Res.* **22**, 5229–5234.
14. Simon, S., Vered, M., Rinehart, A., Cheronis, J. & Janoff, A. (1988). Inhibition of human neutrophil elastase by polyguanylic acid and other synthetic polynucleotides. *Adv. Exp. Med. Biol.* **240**, 65–74.
15. Jaeger, J., Turner, D. & Zuker, M. (1989). Improved predictions of secondary structures for RNA. *Proc. Natl. Acad. Sci. USA* **86**, 7706–7710.
16. Belorgey, D. & Bieth, J.G. (1995). DNA binds neutrophil elastase and mucus proteinase inhibitor and impairs their functional activity. *FEBS Lett.* **361**, 265–268.
17. Navia, M.A., *et al.*, & Hoogsteen, K. (1989). Structure of human neutrophil elastase in complex with a peptide chloromethyl ketone inhibitor at 1.84 Å resolution. *Proc. Natl. Acad. Sci. USA* **86**, 7–11.
18. Gadek, J. (1992). Adverse effects of neutrophils on the lung. *Am. J. Med.* **92**, 27S 31S.
19. Wortel, C. & Doerschuk, C. (1993). Neutrophils and neutrophil–endothelial cell adhesion in adult respiratory distress syndrome. *New Horiz.* **1**, 631–637.
20. Leff, J., *et al.*, & Repine, J.E. (1994). Interleukin-1α-induced lung neutrophil accumulation and oxygen metabolite mediated lung leak in rats. *J. Appl. Physiol.* **266**, 2–8.
21. Guidot, D., Stevens, E., Repine, M., Lucca-Broco, A. & Repine, J. (1994). Intratracheal but not intravascular interleukin-1 causes acute edematous injury in isolated neutrophil-perfused rat lungs through an oxygen radical-mediated mechanism. *J. Lab. Clin. Med.* **123**, 605–609.
22. McDonald, R., Berger, E. & Repine, J. (1987). Neutrophil derived oxygen metabolites stimulate thromboxane release, pulmonary artery pressure increases, and weight gains in isolated perfused rat lungs. *Am. Rev. Respir. Dis.* **135**, 957–959.
23. Benner, S.A., Ellington, A.D. & Tauer, A. (1989). Modern metabolism as a palimpsest of the RNA world. *Proc. Natl. Acad. Sci. USA* **86**, 7054–7058.
24. Tuerk, C. & Gold, L. (1990). Systematic evolution of ligands by exponential enrichment: RNA ligands to bacteriophage T4 DNA polymerase. *Science* **249**, 505–510.
25. Morrison, J.F. & Walsh, C.T. (1988). The behavior and significance of slow-binding enzyme inhibitors. *Adv. Enzymol. Relat. Areas Mol. Biol.* **61**, 201–301.
26. Cha, S. (1975). Tight-binding inhibitors — I. Kinetic behavior. *Biochem. Pharmacol.* **24**, 2177–2185.
27. Segel, I.H. (1975). *Enzyme Kinetics*. John Wiley & Sons, New York.
28. Cantor, C.R., Schimmel, P. (1980). *Biophysical Chemistry*. WH Freeman & Co, New York.

Received: **6 Sep 1995**; revisions requested: **28 Sep 1995**; revisions received: **13 Oct 1995**. Accepted: **16 Oct 1995**.